Dye-sensitized solar cell using a TiO_2 nanocrystalline film electrode prepared by solution combustion synthesis

C.M. Wang and S. L. Chung*

Department of Chemical Engineering, Nation Cheng Kung University, Tainan, 70101, Taiwan, ROC.
n3895115@mai.ncku.edu.tw; slchung@mail.ncku.edu.tw*

Abstract

This investigation was aimed at preparing well performance TiO_2 for dye-sensitized solar cell by solution combustion method. The solution combustion synthesis of TiO_2 powders was investigated over a wide range of synthesis conditions by using metal nitrates (oxidizer)-urea and glycine (fuel) system. Titanium (Ⅳ) n-butoxide was hydrolyzed to obtain titanl hydroxide [$TiO(OH)_2$], and titanyl nitrate [$TiO(NO_3)_2$] was obtained by reaction of $TiO(OH)_2$ with nitric acid. Finally, the aqueous solution containing titanyl nitrate [$TiO(NO_3)_2$] and a fuel,i.e. urea or glycine was combusted to obtain the TiO_2 nanoparticles. The TiO_2 nanoparticles thus obtained were used to fabricate electrodes for DSSC. The performance of the DSSC was measured and compared with those fabricated with commercial TiO_2 powders.

Keywords: dye-sensitized solar cell, solution combustion synthesis, TiO_2

Introduction

Since Honda and Fuijishima found effects of photosensitization of titanium oxide electrode on the electrolysis of water into H_2 and O_2 in 1972, much attention has been focused on the use of the titanium oxide nanoparticles for various technical applications such as electrochromic materials, sterilization, self-cleaning surface, antifogging devices and dye-sensitized solar cells (DSSCs). Dye-sensitized solar cells as a new innovative technology have been developed very quickly during the past decade since Gratzal made a great breakthrough in 1991. In all these devices, the photoelectrode is made of a thin film of nanoparticulate TiO_2. The properties of these films certainly depend on the crystalline phase, morphology and preparation methods that were used, and it is of interest to investigate what kind of film is the most suitable for a specific application and the properties of TiO_2 for making the film.

TiO_2 films can be directly synthesized by a wide variety of techniques such as chemical vapor deposition, sol gel method, hydrothermal processing, microemulsion method, and flame pyrolysis process. Of these methods, the flame pyrolysis processing is a promising technique to synthesize nanometer-sized particles. The flame pyrolysis processing can be completed within a few seconds. This process has many potential advantages such as products obtained directly, low processing cost, energy-efficiency, and high production rate. The flame pyrolysis processing and self-propagating high-temperature synthesis (SHS) are different in approach but equally satisfactory in result.

Solution combustion synthesis (SCS) was developed from self-propagating high-temperature synthesis (SHS) with combination of wet chemical techniques for the synthesis of metal oxide based materials. The process possesses both the advantages of SHS, which utilizes the in-built exothermicity of combustion of the reaction system to directly synthesize the required materials, and the advantages of wet chemical routes, which can produce a compositionally homogeneous mixture making both the ignition temperature and combustion temperature lower than those traditional SHS.

SCS is a flexible technique where oxidizing and reducing precursors are mixed on the molecular level and, under unique conditions of rapid high-temperature reactions, nanoscale powders of desired compositions can be synthesized in one step. The oxidizer (typically nitrates or oxalates) and fuel (e.g., hydrazine, hydrazide, glycine, or urea) are mixed in an aqueous solution to reach molecular level homogenization of the reaction medium. The solution is then heated until self-ignition, yielding a large volume of gas and converting the initial mixture to fine well-crystalline powders of desired compositions. Amomg the advantages of this process are low energy requirements, simple reactor setup, short reaction times, and molecular-scale mixing of precursors, leading to products of desired composition and microstructure.

We have an ongoing research program, which is aimed at investigating mechanisms of combustion synthesis, a novel technique for the synthesis of TiO_2 with a high specific surface area and small band gap that can function under visible light irradiation. The TiO_2 was used to fabricate electrodes for DSSC and was tested for performance.

Experimental

Titanyl nitrate was used as a precursor to prepare the nano-sized TiO_2 by solution combustion method. Titanium (III) n-butoxide was hydrolyzed to obtain titanyl hydroxide. Titanyl nitrate was then obtained by reaction of titanyl hydroxide with nitric acid. Urea or glycine(used as fuels) was added to the aqueous solution of titanyl nitrate and the solution was combusted to obtain TiO_2 particles. For preparation of TiO_2 thin-film, TiO_2 colloical suspensions were prepared by dispersing the TiO_2 particles in distilled water with polyethelene glycol, (PEG, average MW of 20000) as binder. The films were fabricated by dropping the suspension on a transparent conductive oxide glass (TOC) by using a doctor blade technique. The films were then dried at room temperature and then sintered in air at 450℃ for 30min.

The sandwich-type solar cell was assembled by placing a platinum-coated TOC glass (counter electrode)beside the N719 dye-sensitized photoelectrode

(working electrode) and the edges of the cell were sealed with a hot-melt Surlyn spacer (SX 1170-60, Solaronix) by heating it at ~105℃. The redox electrolyte was composed of 0.1M LiI, 0.05M I_2 and 0.6M 1-propyl-2.3-dinethylimidazolium, and was introduced into the cell through two small holes drilled on the counter electrode. The holes were then covered and sealed with a small square sealing sheet of microscope objective glass. The resulting cell had an active area of about 0.25cm^2. The current-voltage characteristics of the cells were measured with a dc voltage current source/monitor (Keithley, 2400). An AM1.5 solar simulator (Oriel, 66983 with a 300W Xenon lamp and an AM1.5 globle filter)was employed as the light source.

The crystalline size and phase of TiO_2 were characterized with X-ray diffraction (XRD, Rigakn, Cu-K α radiation). High resolution, field-emission scanning electron microscope (HEFE-SEM, JSM-6700F, JEOL) was used to examin the film thickness and surface morphology. The surface area and porosity of the nanoporous films were measured by a nitrogen absorption apparatus (Quantachrome NOVA 1000e).

Result and discussion

Combustion synthesis phenomena

A considerable amount of gas was generated during the combustion reaction and thus a certain amount of reaction heat is carried away through convective heat loss. The reaction can proceed in different modes. Smoldering combustion synthesis mode, is characterized by a relatively slow and essentially flameless reaction, leading to slower reaction rates as manifestes in the smoldering combustion behavior. Extremely fast reaction characterized the volume combustion synthesis mode. In this case, the reaction occurs essentially simultaneously in the whole reaction volume. With optimum fuel-to-oxidant ratios, the oxygen contained in the precursor is the main source of oxygen required for combustion reaction. Once the oxygen coming from NO_3^-, is generated, it immediately reacts with urea and oxidizes/consumes most of the fuel, and thus resulting in volume combustion synthesis reaction.

Typical time-temperature profiles of the solution combustion synthesis process when using glycine or urea as fuel are shown in Figure 1and 2, respectively.

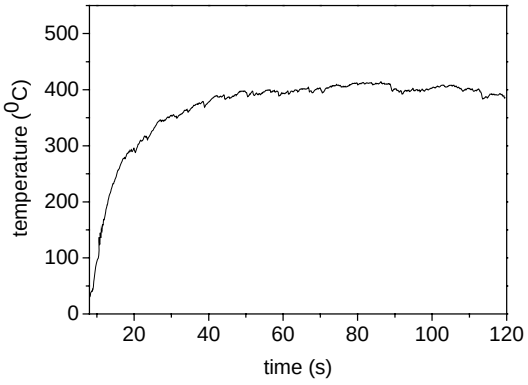

Figure 1. Temperature-time profile when using as fuel glycine

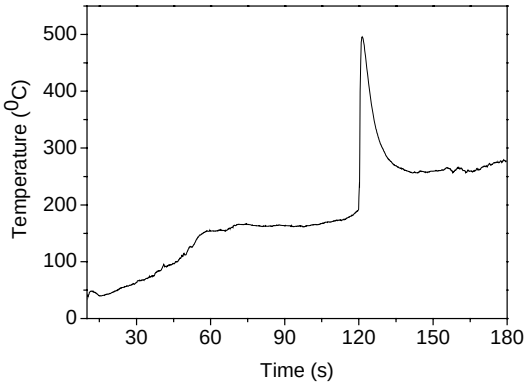

Figure 2. Temperature-time profile when using as fuel urea

The temperature first increased slowly and followed by either a sudden (at ignition temperature, T_{ig}) and uniform temperature rise to a maximum value, T_m(Fig.2), or by essentially constant profile(Fig.1). The former is a typical case of volume combustion synthesis (VCS) mode and the latter the smoldering combustion modes.

Characterization of TiO_2 powders

The variation trend of the BET surface area vs. fuel is listed in Table 1. The solution combustion method would result in gas formation since there is fuel to burn. The fuel acted merely as a space-filling template that dictated the porous structure of the product material, therefore, this combustion synthesis process yielded nanocrystalline powder with a high specific surface area.

Table 1 Effects of fuel on characteristics of TiO_2

Fuel	BET surface area (m^2/g)	crystalline phase	average particle size (nm)
Urea	78.56	Mixed-phase	38±3
Glycine	155.65	anatase	22±3

XRD pattern of solution combustion synthesized TiO_2 was recorded in 2θ range from 20 to 70°. Figure 3. illustrates

the XRD patterns of the samples with different fuels. The pattern of the product when using glycine as fuel can be indexed to pure anatase phase of TiO_2, the rutile phase began to appear when using urea as fuel. The rutile phase of TiO_2 was formed over 600℃ and completely transformed to rutile phase at 800℃. In this study, the rutile phase appears when the maximum combustion temperature reached 500℃, suggesting that the synthesized TiO_2 in this process is unstable perhaps due to existence of carbon in the crystal. The carbon might be introduced from the alkoxide group, urea and improves the transformation of cyystallinity. The carbonaceous species of TiO_2 was detected with XPS, as shown in Figure 4.

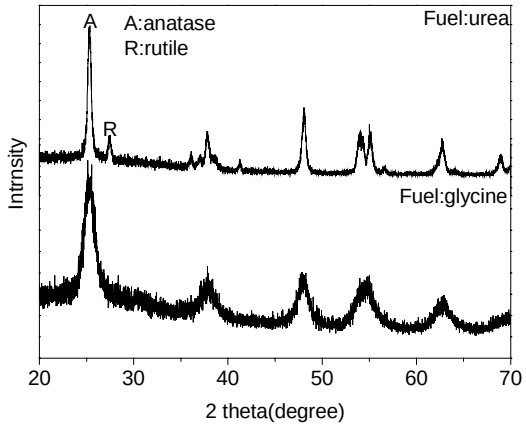

Figure 3. XRD patterns of the synthesized TiO_2

Figure 5 shows C(1s) spectra of combustion synthesized TiO_2. A peak at 285.5eV can be assigned to graphitic carbon and a lower binding energy peak at 284.3eV can be assigned to a carbidic species. Figure 4 shows Ti(2p) core level spectra. Peaks at 459 and 464.8eV indicate that Ti is in 4+ state. Therefore, we concluded that the TiO_2 indeed contains substitution of carbon in the of $TiO_{2-2x}C_xV_{O2}$, where V_{O2} represents the oxide ion vacancy created for charge balance.

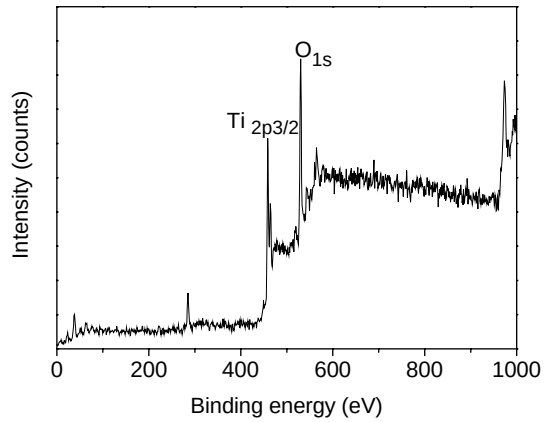

Figure 4. Ti(2p) core level spectra of urea-based TiO_2

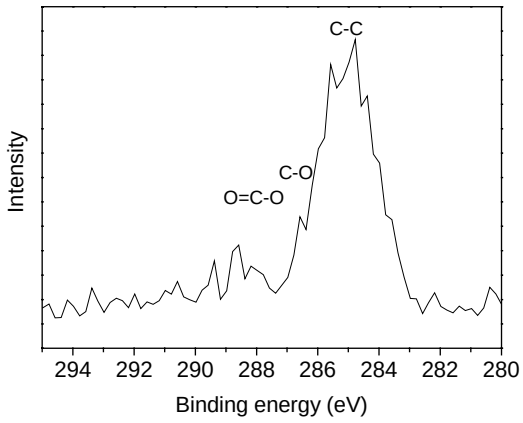

Figure 5. C(1s) spectra of urea-based TiO_2

The microstructure of solution combustion synthesized powder is presented in Figure 6, 7.

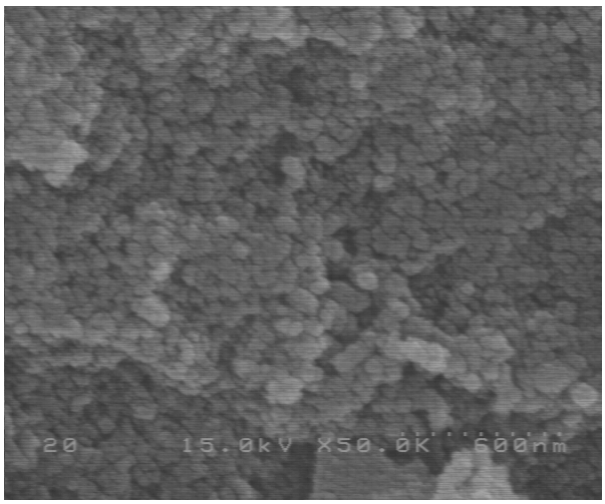

Figure 6. The FE-SEM images of urea-based TiO_2 thin film

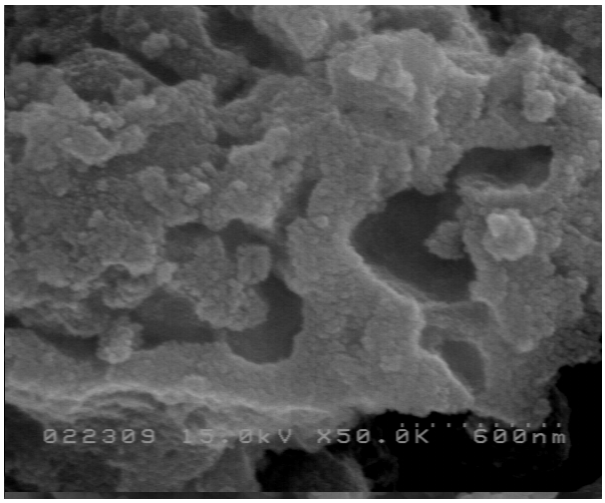

Figure 7. The FE-SEM images of glycine-based TiO_2 thin film

Figure 6 and Figure7 exhibits the FE-SEM images of TiO_2

thin film. Lots of pores are observed on the surface of the film prepared with the TiO_2 when using urea (The maximum combustion temperature is about 500℃) as fuel. (Fig.6) When small primary TiO_2 particles are employed as a starting material for preparing the thin film, the resulting TiO_2 paste is more viscous than that of large primary particles. It indicates that the severe aggregation of primary particles has already occurred before coating, resulting in the larger aggregated particles and pores. It was found that using TiO_2 powder ignition maximum temperature could significantly reduce the aggregation of primary particles during the preparation of TiO_2 slurry. When using glycine as fuel, maximum combustion temperature is about 400℃, the sample results in a uniform thin film. There are no cracks and large aggregated particles as shown in Figure 7.

Photovoltaic performance of DSSC

The ability to control the surface structure of the TiO_2 colloids is important in all the applications that are based on processing related to the colloid surface. One such application is the dye-sensitized solar cell that consists of nanoporous TiO_2 electrode. A comparison between the photovoltaic performance of two cells with electrodes that were fabricated from the two types of colloids shows that the colloids made with glycine as fuel is preferable for dye-sensitized solar cells (Table 2). The compared cells were fabricated using similar procedures and measured under similar conditions in order to extract the contribution of the effect of surface structure. Commercial TiO_2 nanoparticles of P25 and ST01 were also used to fabricate electrodes and the performance of DSSCs were compared. Table 2 summarizes the cell performance data obtained from the I-V curve measurements.

Table 2 The cell performance data

Sample	V_{oc}(V)	J_{sc}(mA/cm^2)	Fill factor(%)	η (%)
P25	0.73	$7.92*10^{-2}$	0.62	0.36
ST01	0.69	$1.83*10^{-1}$	0.69	0.86
Glycine	0.76	$2.15*10^{-2}$	0.60	0.98
Urea	0.66	$1.88*10^{-3}$	0.67	0.82

Glycine-based DSSC exhibits the highest photovoltaic performance compared to the other DSSCs. The overall conversion efficiency(η)of 0.98 for the glycine based DSSC is significantly higher than other based DSSCs. The high crystallinity and uniformity of glycine-based substrate along with the low charge transfer resistance may give rise to the overall conversion efficiency in the glycine-based DSSC. These results imply that the morphology and crystallinity of TiO_2 substrate are essential factors determining the charge transfer characteristics and overall conversion efficiency of the resulting DSSC.

Conclusion

In this work, well performance TiO_2 was synthesized by using solution combustion synthesis. To study the optimum properties in terms of morphological feature, crystallinity, specific area and photovoltaic performance, the TiO_2 nano-particles with high specific area were synthesized by using different fuels. A DSSC fabricated with glycine-based TiO_2 showed the highest photovoltaic performance. This was attributed to the superior morphological features of glycine-based TiO_2, causing the high adsorption of dye and low interface resistance between morphological feature and specific surface area thus photovoltaic performance of TiO_2 particle was found to give rise to the significant enhancement of overall conversion efficiency of DSSC.

References

1. K. Honda, and A. Fujishima, Nature 37, 238 (1972)
2. A. Fujishima, T. N. Rao, and D. A. Tryk, J. Photochemistry and Photobiology C: Photochemistry Reviews 1, 1 (2000)
3. H. Furube, T. Asahi, H. Masuhara, H. Yamashita, and M. Anpo, Chem. Phys. Lett. 336, 424 (2001)
4. R. Asahi, T. Morikawa, T. Ohwaki, K. Aoki, and Y. Taga, Science 269, 293 (2001)
5. S. U. M. Khan, M. Al-Shahry, and W. B. Ingler, Science 2243, 297(2002)
6. Peter Erri, Pavol Pranda and Arvind Varma, Ind. Eng. Chem. Res. 43, 3092 (2004)
7. O'Regan, B.;Grätzel, M. Nature, 353, 737 (1991)